Saturation mutagenesis genome engineering of infective **ΦX174** bacteriophage via unamplified oligo pools and golden gate assembly

Matthew S. Faber^{1,#}, James T. Van Leuven^{2,3,#,*}, Martina M. Ederer³, Yesol Sapozhnikov³, Zoë L. Wilson³, Holly A. Wichman^{2,3}, Timothy A. Whitehead^{4,5}, Craig R. Miller^{2,3}

Here we present a novel protocol for the construction of saturation single-site—and massive multi-site—mutant libraries of a bacteriophage. We segmented the Φ X174 genome into 14 non-toxic and non-replicative fragments compatible with golden gate assembly. We next used nicking mutagenesis with oligonucleotides prepared from unamplified oligo pools with individual segments as templates to prepare near-comprehensive single-site mutagenesis libraries of genes encoding the F capsid protein (421 amino acids scanned) and G spike protein (172 amino acids scanned). Libraries possessed greater than 99% of all 11,860 programmed mutations. Golden Gate cloning was then used to assemble the complete Φ X174 mutant genome and generate libraries of infective viruses. This protocol will enable reverse genetics experiments for studying viral evolution and, with some modifications, can be applied for engineering of therapeutically relevant bacteriophages with larger genomes.

Introduction

Predicting the tempo and trajectory of evolutionary change in the complex environments encountered by viruses and bacteria remains a challenge (Holmes 2013, Neher 2013, Lieberman et al. 2014). Understanding such changes are important for fundamental evolutionary studies as well as biotechnology applications like phage therapy for multi-drug resistant bacteria (Dedrick et al. 2019). Two obstacles preventing better predictions are the oversimplification of the environment in experimental evolution studies compared to wild conditions and the vast number of experimentally unexplored

mutational combinations that can occur, even in short adaptive walks and small genomes. Advances in DNA sequencing and synthesis have opened new ways to study microbial evolution and overcome some of these obstacles (Barrick et al. 2013, Fowler et al. 2014). Unfortunately, suitable methods do not exist for generating comprehensive bacteriophage mutant libraries. This technology gap hinders those seeking to engineer phage for biotechnological applications and for those seeking a deeper understanding of how viruses evolve.

Methods for genetically engineering phages have recently been reviewed (Pires et al. 2016) and commonly involve homologous

¹Dept. Biochemistry and Molecular Biology, Michigan State University, East Lansing MI, 48824; ²Institute for Modeling Collaboration and Innovation, University of Idaho, Moscow ID, 83844; ³Dept. of Biological Sciences, University of Idaho, Moscow ID, 83844; ⁴Dept. of Chemical & Biological Engineering; University of Colorado, Boulder, CO 80303; ⁵Dept. of Chemical Engineering & Materials Science; Michigan State University, East Lansing MI, 48824

*MSF and JTV contributed equally to the work
*Corresponding author, jvanleuven@uidaho.edu

recombination and recombineering. While such approaches can be improved by clever incorporation of CRISPR-Cas systems (Kiro et al. 2014, Lemay et al. 2017, Schilling et al. 2018), the overall modest efficiencies largely limits mutagenesis to the generation and single-site mutation of chimeric genomes (Doore and Fane 2015, Doore et al. 2017), gene deletions (Uchiyama et al. 2009), and limited multi-site mutagenesis (Stockdale et al. 2015). A recent approach combines mutagenesis by PCR with degenerate (NNK) primers with in-cell recombination to create variation at specific residues in the tail fiber of T3 phage (Yehl et al. 2019). By contrast, human viruses often have reverse genetics systems in place where comprehensive mutant libraries can be prepared for single genes (Lee et al. 2018) or regions within a gene (Doud et al. 2018, Wu and Qi 2019) using replicative plasmids that encode whole viruses or viral components. Similarly, deep mutational scanning can be performed on plasmid-encoded phage proteins like the MS2 capsid protein (Hartman et al. 2018). As described by Hartman et al. 2018, such experiments can identify mutations that confer useful characteristics, such as MS2 capsid stability mutations that could improve the targeted delivery of therapeutics to particular cellular compartments.

Advances in the technologies for generating mutant libraries, synthesizing DNA, and for the assembly of large DNA fragments (van Dolleweerd et al. 2018) allow for the construction and assembly of user-defined mutagenesis of long nucleic acids. Nicking mutagenesis (NM) can be used to construct comprehensive single-site or other user-defined mutant libraries (Wrenbeck et al. 2016) using dsDNA as a template. In NM, oligos encode the desired mutations by mismatch with the parental template. On-chip ink-jet printed oligo pools have been integrated into NM (Medina-Cucurella et al. 2019), so one can now construct heterogeneous libraries of oligos that contain tens to hundreds of thousands of high fidelity, unique sequences (Kosuri and Church 2014, Medina-Cucurella et al.

2019) with a low per base pair cost.

We therefore suspected that large userdefined libraries of phage could be generated by combining the advantages of replicative plasmids with advances in DNA synthesis. The bacteriophage ΦX174 is an excellent system to test this approach. High resolution X-ray crystallography structures of the capsid and spike proteins (McKenna et al. 1992, Dokland et al. 1997) are available for ΦX174, making it amenable to compare empirical mutagenesis results and molecular modeling predictions, it has a very small genome (Sanger et al. 1978) of 5,386 nucleotides that is readily sequenced, and it is easily grown on a variety of lab *E. coli* strains. These attractive features of the ΦX174 experimental system have led to proof-of-principle demonstrations from other groups for synthetic genome assembly from oligonucleotides (Smith et al. 2003) and complete refactoring of the phage (Jaschke et al. 2012, Jaschke et al. 2018).

ΦX174 has also been extensively studied (Aoyama et al. 1981, Hafenstein and Fane 2002, Bernal et al. 2004, Rokyta et al. 2006), especially as a model system for experimental evolution (Bull et al. 1997, Crill, Wichman, and Bull 2000, Wichman, Millstein, and Bull 2005) since populations grow rapidly to very large size, mutation rate is high, and the fitness differences between even single mutations can be very large. One of the focal areas of work on ΦX174 and related microvirid phage has been testing models of adaptive evolution and epistasis with empirical data (Rokyta et al. 2005, Caudle, Miller, and Rokyta 2014, Sackman and Rokyta 2018). The inferential power of these studies has been limited by the modest sizes of the mutational libraries.

Here we have combined Golden Gate assembly, nicking mutagenesis, and oligo pool technology to construct near comprehensive single-site and expansive multisite mutant libraries for the genes encoding the capsid F protein and

spike G protein of the bacteriophage ΦX174. To our knowledge this is the first time near comprehensive single site mutant libraries of full capsid and spike proteins have been generated for an infective bacteriophage.

Results

Our strategy for generating large user-defined mutagenesis libraries of bacteriophage ФX174 is shown in Figure 1. The circular 5386 nucleotide genome compactly encodes 11 genes where the F and G genes encode the capsid and spike

proteins, respectively (Fig. 1A). The genome was segmented onto 14 separate plasmids, including 3 plasmids for the F gene and 2 for the G gene (Fig. 1B). Fragment boundaries were first engineered to divide large genes, separate regulatory regions from protein coding genes, and result in fragments of similar size. Initial attempts to clone some fragments resulted in low plasmid yield, presumably due to gene toxicity. These genes were further divided and tested empirically, resulting in the final set of 14 fragments. User-defined comprehensive mutations on F and G were encoded using

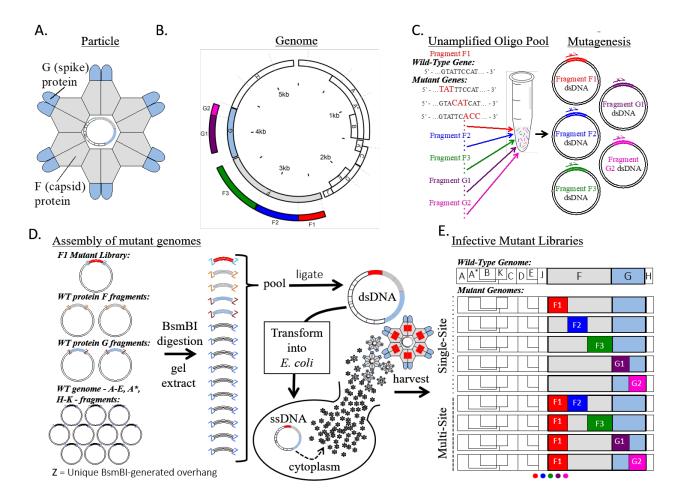
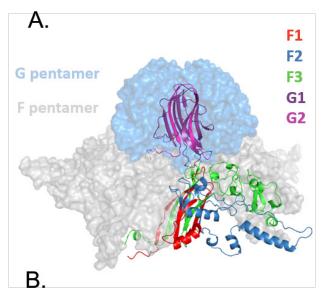
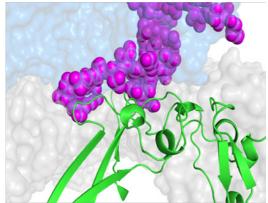


Figure 1. ΦX174 mutant library assembly. A. . Cartoon structure of the ΦX174 virion. F and G proteins are organized into pentamers and are the only exposed proteins in the mature virion. **B.** A linear schematic of the circular ΦX174 genome showing the size and location of the synthetic genome fragments. The location of mutated residues in genes F and G are indicated. **C.** An oligo pool containing all mutagenic oligos for genes F and G was generated and used in Nicking Scanning Mutagenesis for the generation of saturation mutant libraries for genes F and G. **D.** Golden Gate cloning was used to assemble the mutant genomes, which were transformed into XL1-Blue competent cells (Agilent) and plated on susceptible *E. coli* C cells. The resulting plaques were sequenced. **E.** Linear schematics depicting some of the possible mutant libraries that can be generated using the workflow and existing libraries.





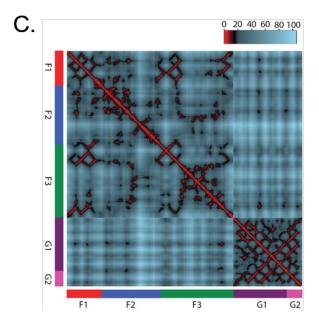


Figure 2. Structural view of potential epistatic interactions between F and G libraries. A. Pentameric complex between F and G shown in surface view. For both F and G, one monomer is shown as a ribbon color-coded according to the saturation mutagenesis library prepared in this work.

B. Close-up of interaction surface between the F3 sub-library of F protein (green ribbons) and G2 sub-library of G protein (purple spheres). C. Distance mapping between alpha carbons in F and G crystal structure. Residues within 10 angstrom are colors red, 10-20 are black, and >20 are blue. Euclidian distances calculated from F-G crystal structure. Heatmap shows that many opportunities exist for close proximity (interactions) both within and between fragments.

nicking mutagenesis with a single unamplified oligo pool containing all 11,860 mutagenic oligonucleotides (Fig. 1C). Φ X174 mutant genomes were reconstituted from individual plasmids using Golden Gate cloning and transformation into a host *E. coli* strain (Fig. 1D). Harvested phages contained all possible nonsynonymous mutations in the F and G genes depending on the mutagenized segments used for Golden Gate cloning (Fig. 1E).

We sought a reverse genetics system for ΦX174 wherein the virus chromosome was segmented and encoded on individual vector plasmids. Our method of construction closely followed that for the assembly of human coronavirus NL63 (Donaldson et al. 2008), where each plasmid contained unique BsmB1 type IIS restriction endonuclease sites flanking unique five nucleotide overlaps of wild-type (WT) ΦX174. This architecture allows for faithful and easy assembly of the complete genome via Golden Gate cloning. The ΦX174 genome was separated into 14 separate nontoxic fragments by PCR and cloned into vector plasmids where genes were separated from their promoters and larger genes were segmented (full sequences for all plasmid inserts are given in Supplemental Note S1). The segments ranged from 129 to 634 base pairs in length, with necessary additional truncations of genes D and A. Φ X174 phage could be reconstituted by digesting pooled plasmids with BsmB1, ligating inserts overnight, and transforming into electrocompetent E. coli C

Table 1. Mutant library NGS statistics. Summary table of the plasmid libraries prior to viral genome assembly.

Fragment	F1	F2	F3	G1	G2
Residues	1-95	99-242	246-427	2-133	136-175
Sequencing reads post quality filter	1,163,959	2,396,395	1,557,554	1,717,075	813,221
Fold oversampling of codon					
combinations	441.1	792.5	412.1	619.4	821.9
Percent of reads with:					
No nonsynonymous mutations	23.0%	33.1%	29.7%	33.3%	25.2%
One nonsynonymous mutation	52.6%	37.4%	35.5%	38.9%	59.7%
Multiple nonsynonymous mutation	24.4%	29.4%	34.7%	27.7%	15.1%
Coverage of possible single nonsynonymous mutations	100%	99.9%	100%	99.8%	100%

cells.

The F and G genes were targeted for saturation mutagenesis. We introduced mutations by nicking mutagenesis, which requires the presence of a BbvCl nicking site on the dsDNA plasmid. The F gene plasmid F3 encoding residues 246-427 of the F gene product contained a unique BbvCl sequence, while the remaining four plasmids (F1, F2, G1, G2) required introduction of BbvCl nicking sites in the vector backbone. The presence in each plasmid of the unique BbvCl nicking site was verified with the successful generation of circular ssDNA from the modified plasmids by BbvCl.Nt and exonuclease digestion (Supplemental Figure S1).

In nicking mutagenesis, desired mutations are introduced by libraries of mutagenic oligonucleotides, which can be sourced from unamplified oligo pools (Medina-Cucurella et al.

2019). We synthesized a custom pool of 11,860 oligos that encoded nearly every missense and nonsense mutation in the F and G genes. Each missense or nonsense mutation was encoded by a single oligonucleotide. Application of nicking mutagenesis using this oligo pool for different plasmids (F1, F2, F3, G1, G2) resulted in at least 14-fold excess transformants required for 99.9% theoretical coverage of the desired library (Supplemental Table S3). The diversity of the mutant plasmid libraries was validated using deep sequencing on an Illumina MiSeg platform. All plasmid libraries have >99.7% coverage of all possible single mutations (n = 11,821/11,860, minimum counts for a mutation >5, full library statistics are given in Table 1 and Supplemental Table S4). Heatmaps showing mutation-specific frequencies for all segments are shown in Supplementary Figures S2-S9.

Mutant dsDNA libraries were transformed into

Table 2. Characterization of viable virus genotypes in mutant phage library. Summary table of number of possible viruses, number of viable viruses recovered from one transformation, and the number of mutant and wildtype genotypes recovered. No mutant genotypes were observed more than once.

Fragment	F1	F2	F3	G1	G2	WT
Possible mutants	1,900	2,880	3,640	3,4	40	NA
Viable transformants	2,300	460	5,840	19,200		6,400
Plaques sequenced	34	25	30	60		30
Wildtype plaques	17 (50%)	11 (44%)	15 (50%)	30 (5	50%)	30 (100%)

non-susceptible hosts (Agilent XL1-Blue), then plated on susceptible hosts (E. coli C) after a 30-minute recovery in SOC. Viral titers increase rapidly after 30 minutes, suggesting that the XL1-Blue cells do not burst until after this time point (Supplemental Table S5). Accordingly, we reasoned that the number of plagues at 30 minutes represents the number of XL1-Blue cells that were transformed with viable genomes. The number of transformants varied considerably between constructs (Table 2). 19,200 plagues were recovered from the co-transformed G1/ G2 libraries, where only 3,480 total variants were expected in the pool. On the contrary, 460 plagues were observed for the F2 library, when 2,280 total variants were in the starting plasmid pool. The underrepresentation of the F2 library at this scale could be remedied by transforming more competent cells. We expect that differences between fragments in the number of recovered viruses is due to in part to the tolerability of fragments to mutation, as inviable mutants would not form plaques. Estimates from deep mutational scanning of model proteins show that approximately 18-38% of all mutations are nonviable (Firnberg et al. 2014, Faber et al. 2019), and this percentage may be larger for structural proteins like F and G.

To test the validity of the mutagenesis and phage reconstitution method, we picked about 30 plaques generated from each library to Sanger sequence. Of these, 40-50% were wildtype and the remaining contained exactly one mutation (Table 2). No variants were observed more than once, supporting the deep sequencing results showing that the libraries consist of thousands of variants. Interestingly, none of the exact substitutions in these sequences have been previously observed (Supplementary Table S6), although mutations at the same residues (G106, F29, F45, F84, F185, F204, F205, and F393) have been seen in previous experiments (Wichman and Brown 2010). In all cases the percentage of WT plaques is slightly higher than in the starting plasmid pools (p-values F1: 0.001, F2: 0.088, F3: 0.015, G: 0.001 1-tailed binomial distribution),

consistent with purifying selection against mutations (Table 1). In contrast, for the control where all plasmids in the Golden Gate reaction were WT, 0% (0/30) plaques contained mutations in the encoded regions.

Discussion

Here we present a novel method for generating comprehensive single-site and multi-site saturation mutant libraries of the spike and capsid proteins of the bacteriophage ФX174. This method uses unamplified oligo pools, nicking scanning mutagenesis, and Golden Gate cloning of the fragmented genome.

The fragment-based system provides an ideal way to generate libraries for the study of epistasis and multi-mutational step regions of the neighborhood around wild type. When a gene is in multiple fragments, the number of mutational variants we expect from the assembled mutant fragments is the product of their individual variant number. Hence, since G1 contains 2640 variants and G2 contains 800 variants, they can be combined to generate 2.1 million double mutation variants. Further, nothing requires the fragments to be from the same gene. For example, since the F and G proteins bind to each other to form the capsid of phiX174 (Fig. 2), libraries combining mutations in F with mutations in G will capture mutations that can readily interact in the protein and have the potential to generate interesting instances of epistasis (Fig 2). The central challenge then becomes how to survey the vast size of these combinatorial plasmid libraries. Right now, our transformational efficiencies vary, but even at the upper end of hundreds of thousands of transformants per reaction, only a fraction of the total diversity in the library can be surveyed.

We are fortunate that our model virus has a small genome, under 6,000 nts, which enabled us to assemble the 14 non-toxic fragments with sufficient transformants for near-complete coverage of the user-defined mutations. This method can be applied with little modification to other phages with small genomes like the microviridae. However, most biotech-relevant phages have larger genomes, and extension of this method to other viruses would encounter the following technical challenges. First, increasing genome sizes decrease transformational efficiencies, and larger genomes have increased susceptibility to DNA shearing (Rogers and Bendich 1988). Both sizedependent effects can disrupt the integrity and coverage of the phage libraries (Edwards and Rohwer 2005). Second, our method includes restrictions on the DNA sequences that can be used. Golden Gate cloning requires a genome without unique Type IIS restriction sequences, while nicking mutagenesis requires that there be only one orientation of the BbvCl nicking site within the template DNA fragment. Third, ligating 14 fragments is close to the upper limit of Golden Gate cloning. Additionally, increasing the size of individual fragments is difficult as the presented method depends on replicating plasmids in E. coli, and larger fragments are more likely to be toxic in vivo.

Based on the above considerations, adapting this method to larger viruses will require modifications for the genome assembly steps. There are a variety of methods available for attempting to improve genome library assembly and amplification. For improving genome assembly, we speculate that a combination of hierarchical assembly (Lee et al. 2015) with other yeast-based assembly methods (Ando et al. 2015) will allow for large viral genomes to be efficiently assembled. Yehl et al. 2019 build large libraries at targeted epitope regions by combining methods; plasmid-based mutagenesis and cloning followed by recombination with wild-type phage during infection. Finally, we speculate that the Tx.Tl cell free expression system (Garamella et al. 2016) will be able to produce the viral libraries with less bias than in vivo amplification in E. coli. In summary, we have presented a method for efficient deep mutational scanning of the bacteriophage Φ X174. We anticipate that this

method will find utility in fundamental molecular evolution studies as well as translate to potential medicinal applications.

Methods

Reagents

All purchased enzymes and DNA purification kits were from New England Biolabs, antibiotics were purchased from GoldBio, other chemicals were purchased from Sigma-Aldrich. Individual primers were purchased from Integrated DNA Technologies.

Segmentation of the Φ X174 genome A phage assembly platform for ΦX174 was devised following (Donaldson et al. 2008). The ΦX174 chromosome was divided into 14 genomic fragments designed to avoid host cell toxicity by separating genes from their promoters and breaking large genes into multiple segments (Supplemental Note S1). Each segment is flanked by unique five nucleotide overlaps of WT ΦX174 sequence so that they can be amplified from the ancestral ΦX174 using PCR primers designed to incorporate terminal BsmB1 restriction sites. Amplicons were cloned into pCR2.1 using the Invitrogen TOPO TA cloning system (Life Technologies, Grand Island, NY) and verified by Sanger sequencing.

Introduction of nicking site

The gene fragments – F1, F2, G1, G2 – in the pCR2.1-TOPO plasmid (Supplemental Notes S1 and S2) had the BbvCl nicking site introduced via overhang PCR, type I restriction enzyme cutting, and ligation. First, PCR was performed with overhang primers (Supplemental Table S1) to introduce the BbvCl site. Standard Phusion Polymerase HF reaction conditions were used with 4 ng of template DNA, cycling conditions as follows: 98°C - 1 min, 25x cycles of: 98°C – 10 seconds, 67°C 15 seconds, 72°C 2.5 minutes, followed by 72°C for 10 minutes. PCR products were run on a 1% agarose gel stained with SYBR™ safe stain (Invitrogen) and the DNA bands at ~4600 bp were extracted using a Monarch® DNA

Gel Extraction Kit. Next, 1 µg of the PCR product was digested with KpnI (20 U) in NEB Buffer 1.1 at 37°C for two hours. Digested DNA was cleaned and concentrated with a Monarch® PCR and DNA Clean and Concentrate Kit and eluted into 20 µL nuclease free H2O. One microliter of the purified and digested DNA was ligated using T4 DNA ligase at ~25°C for 1 hour in standard conditions in a 20 µL reaction. Five microliters of the ligation reaction were transformed into chemically competent XL1-Blue E. coli via standard protocols. Cells were plated on LB agar containing 100 µg/mL carbenicillin and 50 µg/ mL kanamycin and grown at 37°C for ~16 hours. Cells were picked from transformation plates and grown in 50 mL TB with 100 µg/mL carbenicillin and 50 µg/mL kanamycin for ~12 hours, cells were pelleted, and DNA purified using compact midi-preps.

Construction of single site mutant libraries Comprehensive mutant libraries were generated using nicking mutagenesis (NM) as in Wrenbeck et al. 2016 with modifications for using oligo pool mutagenic primers as noted in Medina et al. 2019. A single oligo pool encoding for all possible single missense and nonsense substitutions in F and G was designed using the custom python scripts from Medina et al. 2019 and custom synthesized by Agilent (full sequences of all oligos are given in the associated file "VMA_supplemental_data. csv"). Oligo pools were designed with 20-24 bases of gene overlap flanking the mutated codon. Codons were chosen based on E. coli codon usage frequency, where the highest frequency codon that encoded the mismatch mutation was selected. We printed 14,853 unique oligos, where $14,853 = 12,453 \Phi X 174$ primers – 2,400 other primers. These oligos encode WT (593 primers) and all 20 possible single point mutations (including stop) (11,860 primers). This oligo pool was used directly in NM without further amplification using 2 µg of the relevant golden gate plasmid as a template. Libraries were electroporated into high efficiency electrocompetent XL1-Blue E. coli (Agilent cat #:

200228) using 1 mm electroporation cuvettes at 1200V using a Eppendorf Eporator. Cells were plated on large bioassay plates (245mm x 245mm x 25mm, Sigma-Aldrich) containing LB agar + 100 μ g/mL carbenicillin and 50 μ g/mL kanamycin and grown at 37°C for ~16 hours. Plates were scraped in 10 mL plain LB, broken into ~1.2 mL aliquots, pelleted, and stored -80°C. DNA was purified from 1x aliquot using a Monarch® Plasmid Mini-Prep Kit.

Illumina sequencing prep and analysis Purified library DNA was prepared for deep sequencing as in Kowalsky et al. (2015) using the primers listed in Supplemental Table S2 and gene tiling as specified in Table 1. DNA was Illumina sequenced on a Mi-Seq platform with 250 BP paired end reads. The University of Colorado BioFrontiers Sequencing Core performed the Illumina sequencing. Data was processed using PACT (Klesmith and Hackel 2018) to determine the library coverage with the following changes to the default options in the configuration file: fast_filter_translate: gaverage = 20, glimit = 0; enrichment: ref count threshold = 5, sel count threshold = 0, strict count threshold = True. Library coverage statistics are shown in Supplemental Table S3 and S4.

Assembly of mutant genomes

We pooled plasmid DNA containing all 14 of the phage DNA fragments (500 ng each) and digested them with BsmB1 (Fermentas Fast Digest, Life Technologies, Grand Island, NY) for 30 minutes to 1 hour at 37°C. The digested plasmids were subjected to agarose gel electrophoresis for 10 to 15 minutes using a 1.2% agarose gel to separate the vector from the inserts. The inserts were excised from the gel, purified using the GeneJET gel extraction kit (Fermentas), ligated overnight at 14°C with T4 DNA ligase (Promega Corporation, Madison, WI), and transformed by electroporation into 50 µl of XL1-Blue electocompetent cells. The transformation mix was resuspended with 950 µl of SOC and either plated immediately or incubated for up to 120 minutes (Supplemental Table S5) at 37°C in the

presence of DNase1 (Supplemental Figure S10) to allow for cell lysis and the removal extracellular DNA, respectively. Aliquots of the cell lysates were added to 3 ml of ΦLB top agar containing 50 µl log-phage E. coli C cells and plated onto a ΦLB agar plate. After four to five hours of incubation at 37°C, recombinant phage plagues were visible and plates were removed from the incubator. To verify that the recombinant phage encoded the intended sequence, we picked about 30 plagues for each intended mutational target and Sanger sequenced the entire targeted gene. We also sequenced the F and G genes for about 30 wildtype plaques to assure that no mutations were naturally accumulating. Briefly, individual plaques were picked with sterile toothpicks and placed in 200 uL OLB and gently swirled. 1 uL of this mix was used to PCR amplify approximately ½ of the ΦX174 genome using ΦX-0F (5'-GAGTTTTATCGCTTCCATG-3') and ΦX-2953R (5'-CCGCCAGCAATAGCACC-3') primers. Internal sequencing primers ΦX-979F (5'-CGGCCCCTTACTTGAGG-3') and ΦX-1500R (5'-TTGAGATGGCAGCAACGG-3') were used to sequence gene F. ΦX -2953R was used to sequence gene G. PCR cleanups and sequencing was done at Eurofins Genomics. PCR reaction conditions were: 5 uL10X Tag buffer, 2.5 uL 10 uM ΦX-0F primer, 10 uM ΦX-2953F primer, 0.8 uL 12.5 uM dNTPs, 0.5 uL Tag polymerase (NEB #M0273), 1 uL template, 37.7 uL H20. Thermocycling conditions were 1 cycle at 95°C for 2 min, 30 cycles at 95°C for 15 sec, 52°C for 30 sec, 68°C for 2 min, 1 cycle at 68°C for 5min.

Acknowledgements

We thank the members of the Whitehead, Wichman, and Miller labs for feedback and assistance in composing this work. We especially thank LuAnn Scott for experimental expertise on the ФX174 system. This work was supported by the National Science Foundation BEACON Centre for the Study of Evolution in Action and an NSF EPSCoR T2 under award numbers DBI-0939454 and OIA-1736253 and the National Institute of General Medical Sciences of the National

Institutes of Health under award numbers P20GM104420 and R01GM076040. The content is solely the responsibility of the authors and does not necessarily represent the official views of the National Institutes of Health.

Data Availability

Raw sequencing reads for the truncated mutant libraries have been deposited in the SRA database: SAMN12660301-SAMN12660308. The processed data is available in the supporting information. Additionally, the oligo pool sequences, input files for generating the oligo pool, and an example of the command line input to execute the script from Medina-Cucurella et al. (2019) are available in the Supplemental Information associated with this paper.

References

Ando, H., Lemire, S., Pires, D.P., Lu, T.K. (2015) Engineering modular viral scaffolds for targeted bacterial population editing. Cell Systems 1:187-196.

Aoyama, A., Hamatake, R.K., Hayashi, M. (1981) Morphogenesis of ΦΧ174: in vitro synthesis of infectious phage from purified viral components. Proc. Natl. Aca. Sci. USA 12, 7285-7289.

Barrick, J.E., Lenski, R.E. (2013) Genome dynamics during experimental evolution. Nat Rev Genetics 14:827-839.

Bernal, R.A., Hafenstein, S., Esmeralda, R., Fane, B.A. (2004) Rossmann, M.G. The ΦX174 protein J mediates DNA packaging and viral attachment to host cells. J. Mol. Biol. 337, 1109-1122.

Bull, J.J., Badgett, M.R., Wichman, H.A., Huelsenbeck, J.P., Hillis, D.M., Gulati, A., Ho, C., and Molineux, I.J. (1997) Exceptional Convergent Evolution in a Virus. Genetics 147, 1497–1507.

Caudle, S.B., Miller, C.R., and Rokyta, D.R. (2014) Environment Determines Epistatic Patterns for a ssDNA Virus. Genetics 196, 267–279.

Dedrick, R.M., Guerrero-Bustamante, C.A., Garlena, R.A., Russell, D.A., Ford, K., Harris, K., Gilmour, K.C., Soothill, J., Jacobs-Sera, D., Schooley, R.T., Hatfull, G.F., Spencer, H. (2019) Engineered bacteriophages for treatment of a patient with a disseminated drug-resistant Mycobacterium abscessus. Nature Medicine 25, 730-733.

Dokland, T., McKenna, R., Ilag, L.L., Bowman, B.R., Incardona, N.L., Fane, B.A., Rossmann, M.G. (1997) Structure of a viral procapsid with molecular scaffolding. Nature 389, 308-313.

Donaldson, E.F., Yount, B., Sims, A.C., Burkett, S., Pickles, R.J., Baric, R.S. (2008) Systematic Assembly of a Full-Length Infectious Clone of Human Coronavirus NL63. J. Virol. 82, 11948–11957.

Doore, S.M., Fane, B.A. (2015) The kinetic and thermodynamic aftermath of horizontal gene transfer governs evolutionary recovery. Mol. Biol. Evo. 32, 2571-2584.

Doore, S.M., Schweers, N.J., Fane, B.A. (2017) Elevating fitness after a horizontal gene exchange in bacteriophage ФX174. Virology 501, 25-34.

Doub, M.B., Lee, J.M., Bloom, J.D. (2018) How single mutations affect viral escape from broad and narrow antibodies to H1 influenza hemagglutinin. Nature Comm. 9, 1386.

Edwards, R.A, Rohwer, F. (2005) Viral metagenomics. Nature Reviews Micro. 3:504-509.

Faber, M.S., Wrenbeck, E.W., Azouz, L.R., Steiner, P.J., Whitehead, T.A. (2019) Impact of in vivo protein folding probability on local fitness landscapes. Mol. Biol. Evo. 10.1093/molbev/msz184

Firnberg, E., Labonte, J.W., Gray, J.J., Ostermeier, M. (2014) A comprehensive, high resolution map of a gene's fitness landscape. Mol. Biol. Evol. 31:1581-1592.

Fowler, D.M., Fields, S. (2014) Deep mutational scanning: a new stype of protein science. Nat. Methods 11:801-807.

Garamella, J., Marshall, R., Rustad, M., Noireaux, V. (2016) The all E. coli Toolbox 2.0: a platform for cell-free synthetic biology. ACS Synth. Biol. 5:344-355.

Hafenstein, S., Fane, B.A. (2002) ΦX174 genome-capsid interactions influence the biophysical properties of the virion: evidence for a scaffolding-like function for the genome during the final stages of morphogenesis. J. of Viro. 76, 5350-5356.

Hartman, E.C., Jakobson, C.M., Favor, A.H., Lobba, M.J., Álvarez-Benedicto, E., Francis, M.B., Tullman-Ercek, D. (2018) Quantitative characterization of all single amino acid variants of a viral capsid based drug delivery vehicle. Nature Comm. 9, 1385.

Holmes, E.C. (2013) What can we predict about viral evolution and emergence? Curr. Opin. in Vir. 3:180-184.

Jaschke, P.R., Lieberman, E.K., Rodriguez, J., Sierra, A., Endy, D. (2012) A fully decompressed synthetic bacteriophage ФX174 genome assembled and archived in yeast. Virology 434:278-284.

Jaschke, P.R., Dotson, G.A., Hung, K., Liu, D., and Endy, D. (2018) Definitive demonstration by synthesis of genome annotation completeness. BioRxiv 455428.

Kiro, R., Shitrit, D., Qimron, U. (2014) Efficient engineering of a bacteriophage genome using the type I-E CRISPR-Cas system. RNA Biol. 11:42-44.

Klesmith, J.R., Hackel, B.J. (2018) Improved mutation function prediction via PACT: Protein Analysis and Classifier Toolkit. Bioinformatics 35(6):2707-2712.

Kowalsky, C.A., Klesmith, J.R., Stapleton, J.A., Kelly, V., Reichkitzer, N., Whitehead T.A. (2015) High-Resolution Sequence-Function Mapping of Full-Length Proteins. PLoS One 10:e0118193.

Kosuri, S., Church, G.M. (2014) Large-scale de novo DNA synthesis: technologies and applications. Nat. Methods 11, 499-507.

Lee, J.M., Huddleston, J., Doud, M.B., Hooper, K.A., Wu, N.C., Bedford, T., Bloom, J.D. (2018) Deep mutational scanning of hemagglutinin helps predict evolutionary fates of human H3N2 influenza variants. Proc. Natl. Aca. Sci. USA 115, E8276-E8285.

Lee, M.E., DeLoache, W.C., Cervantes, B., Dueber, J.E. (2015) A highly characterized yeast toolkit for modular, multipart assembly. ACS Synth. Biol. 4:975-986.

Lemay, M.L., Tremblay, D.M., Moineau, S. (2017) Genome engineering of virulent lactococcal phages using CRIPSR-Cas9. ACS Synth. Biol. 6:1351-1358.

Lieberman, T.D., Flett, K.B., Yelin, I., Martin, T.R., McAdam, A.J., Priebe, G.P., Kishony, R. (2014) Genetic variation of a bacterial pathogen within individuals with cystic fibrosis provides a record of selective pressures. Nature Gen 46:82-87.

McKenna, R., Xia, D., Willingmann, R., Ilag, L.L., Krishnaswamy, S., Rossmann, M.G., Olson, N.H., Baker, T.S., Incardona, N.L. (1992) Atomic structure of single-stranded DNA bacteriophage ΦΧ174 and its functional implications. Nature 355, 137-143.

Medina-Cucurella, A., Steiner, P.J., Faber, M.S., Beltrán, J., Borelli, A., Kirby, M.B., Cutler, S.R., Whitehead, T.A. (2019) User-defined single pot mutagenesis using unpurified oligo pools. Prot. Eng. Des. Sel. 32(1)41-45.

Neher, R.A. (2013) Genetic draft, selective interference, and population genetics of rapid adaptation. Annu. Rev. Ecol. Evol. Syst. 44:195-215.

Pires, D.P., Cleto, S., Sillankorva, S., Azeredo, J., Lu, T.K. (2016) Genetically engineered phages: a review of advances over the last decade. Microbiol. and Mol. Biol. Rev. 80:523-543.

Rokyta, D.R., Joyce, P., Caudle, S.B., and Wichman, H.A. (2005) An empirical test of the mutational landscape model of adaptation using a single-stranded DNA virus. Nat Genet. 37, 441–444.

Rokyta, D.R., Burch, C.L., Caudle, S.B., Wichman, H.A. (2006) Horizontal gene transfer and the evolution of microvirid coliphage genomes. J. of Bacter. 188, 1134-1142.

Rogers, S.O., Bendich, A.J. (1988) Extraction of DNA from plant tissues. Plant Mole Biol. Manual A6:1-10.

Sackman, A.M., and Rokyta, D.R. (2018) Additive Phenotypes Underlie Epistasis of Fitness Effects. Genetics 208, 339–348.

Sanger, F., Coulson, A.R., Friedmann, T., Air, G.M., Barrell, B.G., Brown, N.L., Fiddes, J.C., Hutchinson, C.A., Slocombe, P.M., Smith, M. (1978) The nucleotide sequence of bacteriophage phiX174. J. Mol. Biol. 125:225-246.

Schilling, T., Dietrich, S., Hoppert, M., Hertel, R. (2018) A CRISPR-Cas9-based toolkit for fast and precise in vivo genetic engineering of Bacillus subtilis phages. Viruses 10:241.

Smith, H.O., Hutchinson III, C.A., Pfannkoch, C., Venter, J.C. (2003) Generating a synthetic genome by whole genome assembly: Φ X174 bacteriophage from synthetic oligonucleotides. Proc. Natl. Aca. Sci. USA 100, 15440-15445.

Stockdale, S.R., Collins, B., Silvia, S., Douillard, F.P., Mahony, J., Cambillau, C., van Sinderen, D. (2015) Structure and assembly of TP901-1 Virion unveiled by mutagenesis. PLoS One 10, e0131676.

Uchiyama, A., Heiman, P., Fane, B.A. (2009) N-terminal deletions of the ΦX174 external scaffolding protein affect the timing and fidelity of assembly. Virology 386, 303-309.

van Dolleweerd, C.J., Kessans, S.A., Van de Bittner, K.C., Bustamante, L.Y., Bundela, R., Scott, B., Nicholson, M.J., Parker, E.J. (2018) MIDAS: a modular DNA assembly system for synthetic biology. ACS Synth Biol 7:1018-1029.

Wichman, H.A., and Brown, C.J. (2010) Experimental evolution of viruses: Microviridae as a model system. Phil. Trans. of the Royal Society B. 365, 2495–2501.

Yehl, K., Lemire, S., Yang, A.C., Ando, H., Mimee, M., Torres, M.D.T., de la Fuente-Nunez, C., and Lu, T.K. (2019). Engineering Phage Host-Range and Suppressing Bacterial Resistance through Phage Tail Fiber Mutagenesis. Cell 179, 459-469.e9. Genetics 170, 19–31.

Supplemental Information for

Saturation mutagenesis genome engineering of infective $\Phi X174$ bacteriophage via

unamplified oligo pools and golden gate assembly

Matthew S. Faber¹, James T. Van Leuven^{2,3}, Martina M. Ederer³, Yesol Sapozhnikov³,

Zoë L. Wilson³, Holly A. Wichman^{2,3}, Timothy A. Whitehead^{4,5}, Craig R. Miller^{2,3*}

Affiliations: ¹Dept. Biochemistry and Molecular Biology, Michigan State University,

East Lansing MI, 48824; ²Institute for Modeling Collaboration and Innovation,

University of Idaho, Moscow ID, 83844; ³Dept. of Biological Sciences, University of

Idaho, Moscow ID, 83844; ⁴Dept. of Chemical & Biological Engineering; University of

Colorado, Boulder, CO 80303; 5Dept. of Chemical Engineering & Materials Science;

Michigan State University, East Lansing MI, 48824

*Correspondence to:

jvanleuven@uidaho.edu

Department of Biological Sciences

875 Perimeter MS 3051

Moscow, Idaho 83844-3051

Note S1: DNA sequences of Φ X174 viral capsid protein gene fragments. Sequences provided span from the 5' EcoRV to the 3' BamHI site (bolded sequences). Mutagenic regions are highlighted in pink, non-mutated coding regions are highlighted in blue, BsmBI sites are highlighted in green. Regions with overlapping protein coding regions on different reading frames are colored dark blue.

>Fragment_F1

GATATCTGCAGAATTCGCCCTTCGTCTCATCAAACGGCCTGTCTCATCATGG
AAGGCGCTGAATTTACGGAAAACATTATTAATGGCGTCGAGCGTCCAGCTAA
AGCCGCTGAATTGTTCGCGTTTACCTTGCGTGTACGCGCAGGAAACACTGAC
GTTCTTACTGACGCAGAAGAAAAACGTGCGTCAAAAAATTACGTGCAGAAGGAG
TGATGTAATGTCTAAAGGTAAAAAACGTTCTGGCGCTCGCCCTGGTCGTCCGC
AGCCGTTGCGAGGTACTAAAGGCAAGCGTAAAGGCGCTCGTCTTTGGTATGT
AGGTGGTCAACAATTTTAATTGCAGGGGCCTTCGGCCCCTTACTTGAGGATAA
ATTATGTCTAATATTCAAACTGGCGCCGAGCGTATGCCGCATGACCTTTCCCA
TCTTGGCTTCCTTGCTGGTCAGATTGGTCGTCTTTATTACCATTTCAACTACTCC
GGTTATCGCTGGCGACTCCTTCGAGATGGACGCCGTTGGCGCTCTCCGTCTTT
CTCCATTGCGTCGTGGCCTTGCTATTGACTCTACTGTAGACATTTTTACTTTTT
ATGTCCCTCATCGTCACGTTTATGGTGAACAGTGGATTAAGTTCATGAAGGAT
GGTGTTAATGCCACTCCTCCCCCCACTGTGAGACCG
AAGGGCGAATTCCAGCA
CACTGGGCGGCCGTTACTAGTGGATCC

>Fragment_F2

GATATCTGCAGAATTCGCCCTTCGTCTCGACTGTTAACACTACTAGGTTATATT
GACCATGCCGCTTTTCTTGGCACGATTAACCCTGATACCAATAAAATCCCTAA
GCATTTGTTTCAGGGTTATTTGAATATCTATAACAACTATTTTAAAGCGCCGT
GGATGCCTGACCGTACCGAGGCTAACCCTAATGAGCTTAATCAAGATGATGC
TCGTTATGGTTTCCGTTGCTGCCATCTCAAAAACATTTGGACTGCTCCGCTTCC
TCCTGAGACTGAGCTTTCTCGCCAAATGACGACTTCTACCACATCTATTGACA
TTATGGGTCTGCAAGCTGCTTATGCTAATTTGCATACTGACCAAGAACGTGAT
TACTTCATGCAGCGTTACCGTGATGTTATTTCTTCATTTGGAGGTAAAACCTC
TTATGACGCTGACAACCGTCCTTTACTTGTCATGCGCTCTAATCTCTGGGGGAG
ACGAAGGGCGAATTCCAGCACACTGGCGGCCCGTTACTAGTGGATCC

>Fragment_F3

TAAAAGATTGAGTGTGAGGTTATAACGCCGAAGCGGTAAAAATTTTAATTTT TGCCGCTGAGGGGTTGACCAAGCGAAGC<mark>GAGACG</mark>AANGGCGAATTCCAGCA CACTGGCGGCCGTTACTAGT**GGATCC**

>Fragment_G1

GATATCTGCAGAATTCGCCCTTCGTCTCCCGAAGCGCGGTAGGTTTTCTGCTTA
GGAGTTTAATCATGTTTCAGACTTTTATTTCTCGCCATAATTCAAACTTTTTT
CTGATAAGCTGGTTCTCACTTCTGTTACTCCAGCTTCTTCGGCACCTGTTTTAC
AGACACCTAAAGCTACATCGTCAACGTTATATTTTGATAGTTTGACGGTTAAT
GCTGGTAATGGTGGTTTTCTTCATTGCATTCAGATGGATACATCTGTCAACGC
CGCTAATCAGGTTGTTTCTGTTGGTGCTGATATTGCTTTTGATGCCGACCCTA
AATTTTTTGCCTGTTTGGTTCGCTTTGAGTCTTCTTCGGTTCCGACTACCCTCC
CGACTGCCTATGATGTTTATCCTTTGAATGGTCGCCATGATGGTGGTTATTAT
ACCGTCAAGGACTGTGTGACTATTGACGTCCTTCCCCGTACGGAGACGAAGG
GCGAATTCCAGCACACACTGGCGGCCGTTACTAGTGGATCC

>Fragment G2/H1

>Fragment H2

>Fragment_H3

GATATCTGCAGAATTCGCCCTTCGTCTCAAAGAAATGACTCGCAAGGTTAGTGCTGAGGTTGACTTAGTTCATCAGCAAACGCAGAATCAGCGGTATGGCTCTTCTCATATTGGCGCTACTGCAAAGGATATTTCTAATGTCGTCACTGATGCTGCTTCTGGTGTGGTTGATATTTTCATGGTATTGATAAAGCTGTTGCCGATACTTG

GAACAATTTCTGGAAAGACGGTAAAGCTGATGGTATTGGCTCTAATTTGTCTA GGA<mark>GAGACG</mark>AAGGGCGAATTCCAGCACACTGGCGCCGTTACTAGT**GGAT**

>Fragment_A1/H

GATATCTGCAGAATTCGCCCTTCGTCTCCTAGGAAATAACCGTCAGGATTGA CACCCTCCCAATTGTATGTTTTCATGCCTCCAAATCTTGGAGGCTTTTTTATGG TTCGTTCTTATTACCCTTCTGAATGTCACGCTGATTATTTTGACTTTGAGCGTA TCGAGGCTCTTAAACCTGCTATTGAGGCTTGTGGCATTTCTACTCTTTCTCAAT CGAGACGAAGGGCGAATTCCAGCACACTGGCGGCCGTTACTAGTGGATCC

>Fragment_A2

>Fragment_A3

GATATCTGCAGAATTCGCCCTTCGTCTCACACTCTCACGTTGGCTGACGACCGATTAGAGGCGTTTATGATAATCCCAATGCTTTGCGTGACTATTTTCGTGATATTGGTCGTATGGTTCTTGCTGCCGAGGGTCGCAAGGCTAATGATTCACACGCCGACTGCTATCAGTATTTTTGTGTGCCTGAGTATGGTACAGCTAATGGCCGTCTTCATTCCATGCGGTGCACTTTATGCGGACACTTCCTACAGGTAGCGTTGACCCTAATTTTGGTCGTCGGGTACGCAATCGCCGCCAGTTAAATAGCTTGCAAAATACGTGGCCTTATGGTTACAGTATGCCCAGAGACGAAGGGCGAATTCCAGCACACTGGCGGCCGTTACTAGTGGATCC

>Fragment A4/B

GATATCTGCAGAATTCGCCCTTCGTTCTCTTTGCCCATCGCAGTTCGCTACACGCA
GGACGCTTTTTCACGTTCTGGTTGGTTGTGGCCTGTTGATGCTAAAGGTGAGC
CGCTTAAAGCTACCAGTTATATGGCTGTTGGTTTCTATGTGGCTAAATACGTT
AACAAAAAGTCAGATATGGACCTTGCTGCTAAAGGTCTAGGAGCTAAAGAAT
GGAACAACTCACTAAAAAACCAAGCTGTCGCTACTTCCCAAGAAGCTGTTCAG
AATCAGAATGAGCCGCAACTTCGGGATGAAAATGCTCACAATGACAAATCTG
TCCACGGAGTGCTTAATCCAACTTACCAAGCTGGGTTACGACGCGACGCCGT
TCAACCAGATATTGAAGCAGAACGCAAAAAAGAGAGATGAGATTGAGGCTGG
GAAAAGTTACTGTAGCCGACAAAAAATGATTGGCGTATCCAACCTGCAG
AGTTTTATCGCTTCCATGACGCAGAAGTTAACACTTTCGGATATTTCTGATGA

GTCGGAGACGAAGGGCGAATTCCAGCACACTGGCGGCCGTTACTAGTGGATCCC

>Fragment_K/C/A

GATATCTGCAGAATTCGCCCTTCGTCTCGAGAAAAATTATCTTGATAAA GCAGGAATTACTACTGCTTGTTTACGAATTAAATCGAAGTGGACTGCTGGCG GAAAATGAGAAAATTCGACCTATCCTTGCGCAGCTCGAGAAGCTCTTACTTT GCGACCTTTCGCCATCAACTAACGAGAGACGAAGGGCGAATTCCAGCACACT GGCGGCCGTTACTAGTGGAT

>Fragment C/K

>Fragment D/C/E

GATATCTGCAGAATTCGCCCTTCGTCTCACACTTTAAAAGAGCGTGGATTACT
ATCTGAGTCCGATGCTGTTCAACCACTAATAGGTAAGAAATCATGAGTCAAG
TTACTGAACAATCCGTACGTTTCCAGACCGCTTTGGCCTCTATTAAGCTCATT
CAGGCTTCTGCCGTTTTGGATTTAACCGAAGATGATTTCGATTTTCTGACGAG
TAACAAAGTTTGGATTGCTACTGACCGCTCTCGTGCTCGCTGCGTTGAGG
CTTGCGTTTATGGTACGCTGGACTTTGTTGGGATACCCTCGCTTTCCTGCTCCTG
TTGAGTTTATTGCTGCCGTCATTGCTTATTATGTTCATCCCGTGAGACG
AAGG
GCGAATTCCAGCACACACTGGCGGCCGTTACTAGTGGAT

Note S2: Amino acid sequences of Φ X174 mutagenized viral capsid protein gene fragments. Only mutagenized regions of gene fragments shown.

>Fragment_F1

MSNIQTGAERMPHDLSHLGFLAGQIGRLITISTTPVIAGDSFEMDAVGALRLSPLR RGLAIDSTVDIFTFYVPHRHVYGEQWIKFMKDGVNATPL

>Fragment_F2

NTTGYIDHAAFLGTINPDTNKIPKHLFQGYLNIYNNYFKAPWMPDRTEANPNELN QDDARYGFRCCHLKNIWTAPLPPETELSRQMTTSTTSIDIMGLQAAYANLHTDQE RDYFMQRYRDVISSFGGKTSYDADNRPLLVMRSN

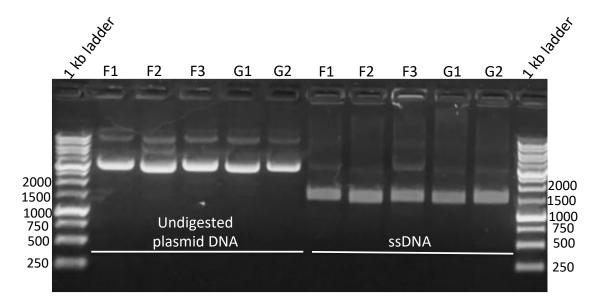
>Fragment F3

SGYDVDGTDQTSLGQFSGRVQQTYKHSVPRFFVPEHGTMFTLALVRFPPTATKEI QYLNAKGALTYTDIAGDPVLYGNLPPREISMKDVFRSGDSSKKFKIAEGQWYRY APSYVSPAYHLLEGFPFIQEPPSGDLQERVLIRHHDYDQCFQSVQLLQWNSQVKF NVTVYRNLPTTRDSIMTS

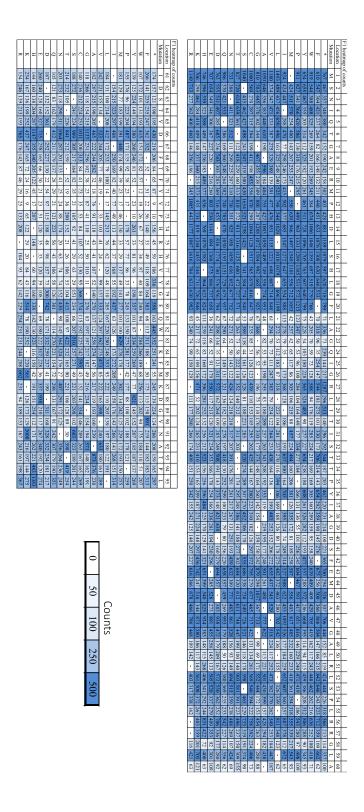
>Fragment_G1

FQTFISRHNSNFFSDKLVLTSVTPASSAPVLQTPKATSSTLYFDSLTVNAGNGGFL HCIQMDTSVNAANQVVSVGADIAFDADPKFFACLVRFESSSVPTTLPTAYDVYPL NGRHDGGYYTVKDCVTIDVLP

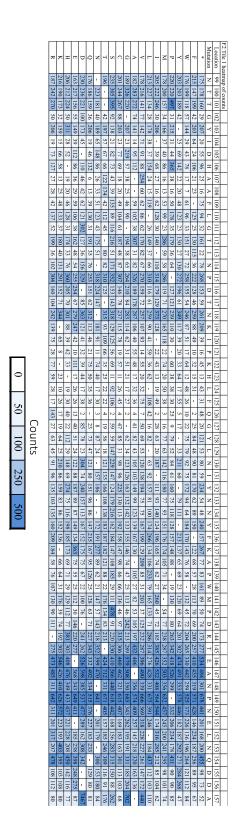
>Fragment_G2
PGNNVYVGFMVWSNFTATKCRGLVSLNQVIKEIICLQPLK



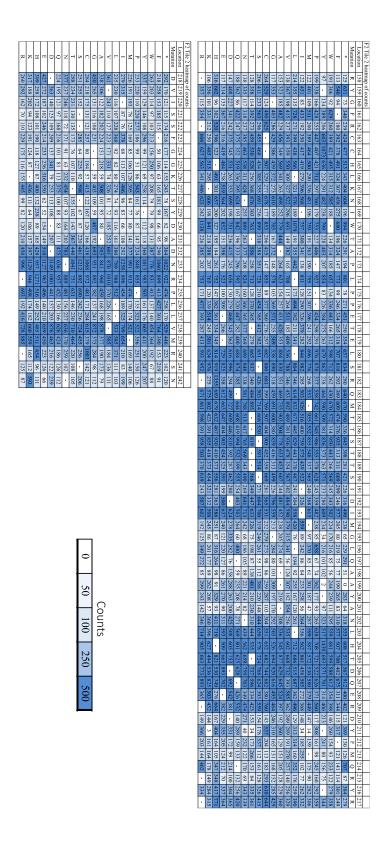
Supplemental Figure S1. Introduction of nicking sites into shuttle vectors containing viral genes. Verification of the introduction of the BbvCI nicking site into the shuttle vector containing the viral genes is shown by the template prep step in the nicking mutagenesis protocol (generation of ssDNA). Samples were run on a 1% agarose gel with SYBRTM Safe DNA gel stain (Invitrogen) added before casting, the ladder used is the 1 kb DNA ladder from GoldBio.



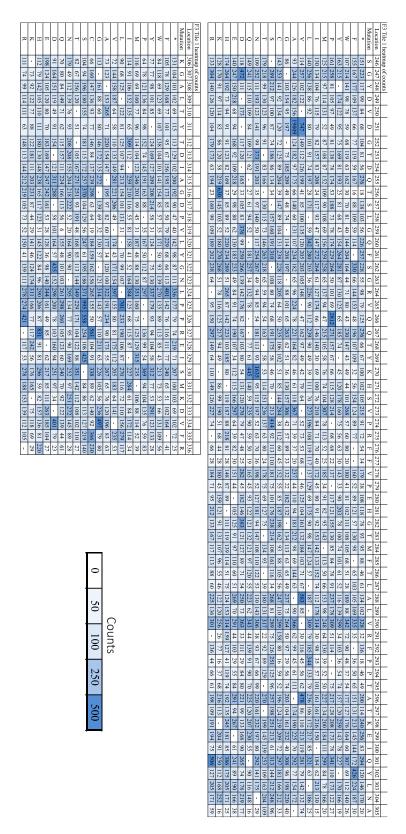
Supplementary Figure S2: F1 heatmap of mutational frequency represented by number of sequencing read counts "counts".



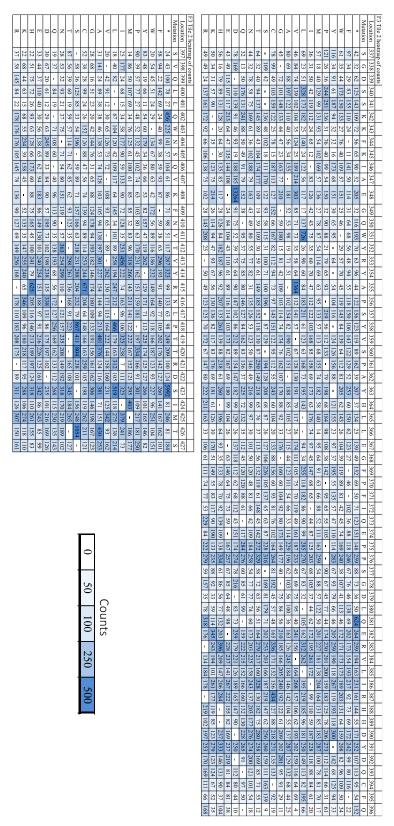
Supplementary Figure S3: F2 tile 1 heatmap of mutational frequency represented by number of sequencing read counts "counts".



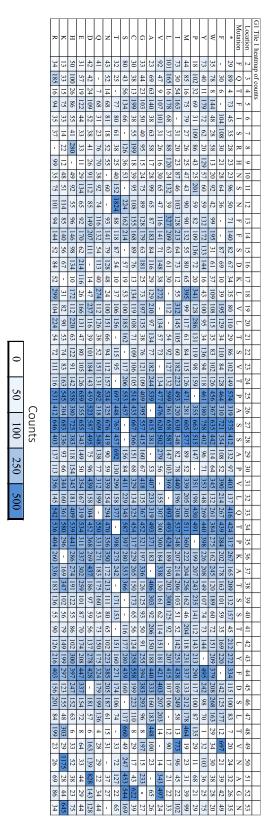
Supplementary Figure S4: F2 tile 2 heatmap of mutational frequency represented by number of sequencing read counts "counts".



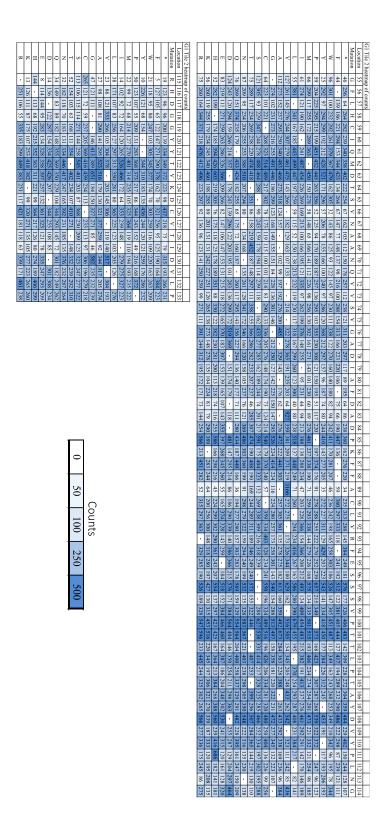
Supplementary Figure S5: F3 tile 1 heatmap of mutational frequency represented by number of sequencing read counts "counts".



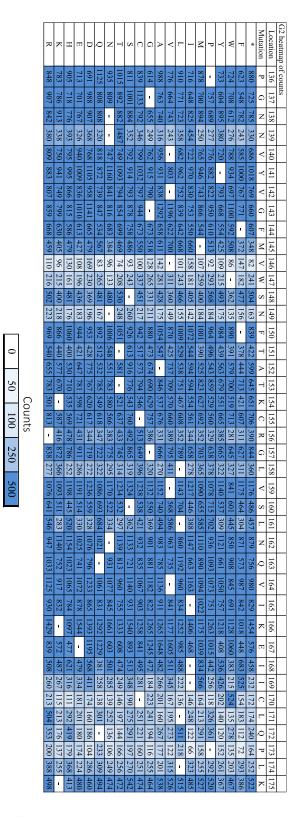
Supplementary Figure S6: F3 tile 2 heatmap of mutational frequency represented by number of sequencing read counts "counts".



Supplementary Figure S7: G1 tile 1 heatmap of mutational frequency represented by number of sequencing read counts "counts".

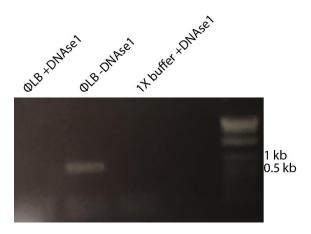


Supplementary Figure S8: G1 tile 2 heatmap of mutational frequency represented by number of sequencing read counts "counts".



Supplementary Figure S9: G2 heatmap of mutational frequency represented by number of sequencing read counts "counts".

Supplementary Figure S10: Agarose gel image showing effectiveness of DNase1 in ΦLB. 25 cycles of PCR were performed after a 1-hour 37°C incubation of WT ligation mix with DNase1. Primer sequences for phix_2375F and phix_2949R were 5'-ACACTGACGACATGGTTCTACAtctgcttaggagtttaatc-3' and 5'-TACGGTAGCAGAGACTTGGTCTgcaccaaacataaatcacc-3'. These primers include annealing sequences for Illumina 2nd round barcoding primers.



Supplemental table S1. Primers for incorporating BbvCI nicking sites into the pCR2.1-topo shuttle vector. Blue text is the overlap region with the shuttle vector, red is the KpnI site, green is the BbvCI site.

Nick_incorporation_fwd
GCTCTACGGGTACCGCTGAGGGAGCTCGGATCCACTAGTAACG
Nick_incorporation_rvs
GCTCTAACGGGTACCAAGCTTGGCGTAATCATGGTC

Supplemental table S2. Inner and outer primers for PCR reactions for Illumina sequencing. Red indicates overhang regions for attaching Illumina adapter primers (inner PCR primers) or overhangs for attaching to inner PCR product (outer PCR primers), black is the overlap region in the gene or the barcode, blue is the Illumina adapter.

Inner PCR Primers	Sequence (5' to 3')
Fragment F1 Fwd	gttcagagttctacagtccgacgacccttacttgaggataaatt
Fragment F2 Tile 1 Fwd	gttcagagttctacagtccgacgatcgactcactatagggcgaa
Fragment F2 Tile 2 Fwd	gttcagagttctacagtccgacgatcagcttaatcaagatgatgct
Fragment F3 Tile 1 Fwd	gttcagagttctacagtccgacgatccgtctctctgggca
Fragment F3 Tile 2 Fwd	gttcagagttctacagtccgacgatcgaaggatgttttccgt
Fragment G1 Tile 1 Fwd	gttcagagttctacagtccgacgatcgaattgggccctctag
Fragment G1 Tile 2 Fwd	gttcagagttctacagtccgacgatcggttaatgctggtaatgg

Fragment G2 Fwd	gttcagagttctacagtccgacgatcggccctctagatgca
Fragment F1 Rvs	ccttggcacccgagaattccattcgtctcacagtcgg
Fragment F2 Tile 1 Rvs	ccttggcacccgagaattccacaacggaaaccataacg
sdFragment F2 Tile 2 Rvs	ccttggcacccgagaattccattcgtctccccagag
Fragment F3 Tile 1 Rvs	ccttggcacccgagaattccatcttagacgaatcaccaga
Fragment F3 Tile 2 Rvs	ccttggcacccgagaattccatcacactcaatcttttatca
Fragment G1 Tile 1 Rvs	ccttggcacccgagaattccatgcaatgaagaaaacca
Fragment G1 Tile 2 Rvs	ccttggcacccgagaattccacttcgtctccgtacg
Fragment G2 Rvs	ccttggcacccgagaattccattgaccgcctcca
Illumina outer primer adapter	aatgatacggcgaccaccgagatctacacgttcagagttctacagtccga
Illumina outer PCR adapters and barcodes	
RPI31 (Fragment F1)	caagcagaagacggcatacgagatATCGTGgtgactggagttccttggcacccgagaattcca
RPI15 (Fragment F2 Tile 1)	caagcagaagacggcatacgagatTGACATgtgactggagttccttggcacccgagaattcca
RPI16 (Fragment F2 Tile 2)	caagcagaagacggcatacgagatGGACGGgtgactggagttccttggcacccgagaattcca
RPI17 (Fragment F3 Tile 1)	caagcagaagacggcatacgagatCTCTACgtgactggagttccttggcacccgagaattcca
RPI18 (Fragment F3 Tile 2)	caagcagaagacggcatacgagatGCGGACgtgactggagttccttggcacccgagaattcca
RPI19 (Fragment G1 Tile 1)	caagcagaagacggcatacgagatTTTCACgtgactggagttccttggcacccgagaattcca
RPI20 (Fragment G1 Tile 2)	caagcagaagacggcatacgagatGGCCACgtgactggagttccttggcacccgagaattcca
RPI21 (Fragment G2)	caagcagaagacggcatacgagatCGAAACgtgactggagttccttggcacccgagaattcca

Supplemental Table S3. Mutant library preparation summary. Summary table of the transformants required for sufficient library coverage, transformants obtained during comprehensive mutant library preparation by nicking scanning mutagenesis, and the fold excess of the number of transformants required for coverage.

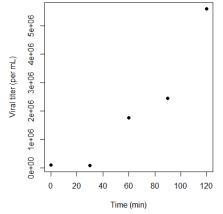
Gene mutated	F1	F2	F3	G1	G2
Number of Residues	95	144	182	132	40
Transformants obtained following NSM	620,000	890,000	370,000	620,000	640,000
Required transformants for 99.9% coverage of possible library	13781	20889	26401	19148	5803
Fold excess over amount required for coverage	45	43	14	32	110

Supplementary Table S4. Mutant plasmid library NGS statistics. Summary table of the libraries prior to viral genome assembly. Long fragments required separate amplicon sequencing reactions as shown.

Fragment	F1	F2		F3		G1		G2
Tile Number	1	1	2	1	2	1	2	1
Residues	1-95	99-157	158-242	246-336	337-427	2-53	55-133	136-175
Sequencing reads post quality filter	1163959	681935	1714460	800377	757177	747800	969275	813221
Fold oversampling of codon combinations	441.1	499.8	851	364.8	345.1	632.8	517.6	821.9
Percent of reads with:								
No nonsynonymous mutations	23.0%	63.3%	52.3%	54.0%	55.0%	68.3%	48.8%	25.2%
One nonsynonymous mutation	52.6%	27.5%	36.3%	33.1%	32.1%	24.1%	39.8%	59.7%
Multiple nonsynonymous	24.40/	0.20/	11 20/	12.00/	12.00/	7 (0)	11 40/	15.10/
mutation Coverage of possible	24.4%	9.2%	11.3%	12.9%	12.8%	7.6%	11.4%	15.1%
single nonsynonymous mutations	100%	100%	99.8%	100%	99.9%	99.6%	100%	100%

Supplemental Table S5. Viral growth rate during transformation cell recovery.

Viral titers immediately after transformation (0 min) and then for every 30 min after up to 2 hours. As the XL1-Blue cells are not susceptible, the increase in titer is the result of cell bursts, which releases viable phage. While the virus is replicating for the first 30 minutes, they are all held within a cell and will only make one plaque.



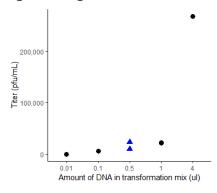
Time	Dilution	#Plaques	Titer
(min)			(viruses/mL)
0	1E-3	101	101,000
30	1E-3	90	90,000
60	1E-4	177	1,770,000
90	1E-4	245	2,450,000
120	1E-5	56	5,600,000

Supplemental Table S6. List of observed mutations in plaque sequencing. Residues where more than one substitution was observed are bolded. Residues where mutations have been observed in previous studies (but not the exact substitution) are indicated*.

Fragment	Mutations
G1	L20T, S28I, Q33N, T34N , T34I , A37S, S46M , S46C , A51L, T64D, A69P,
	V75C, A83S, F87Q, C90Q, S97F, T102M, L103V, A106C* , A106Q* ,
	T122G, V127N
G2	T151G, A152F, T153L, K154A, R156L , R156M
F1	H13M, D14H , D14Q , L15C, S16E, I29G*, M44Q, D45Q*, L52M, F68V,
	G79A, K84V*, D88M, N91T , N91Y , T93E , T93L , T93Y
F2	N134K, T145R, E146D, P149V, E177W, S181N, Q183P, T185S*, L196M,

	H204I*, T205D*, Y211H, S222E, N233R
F3	D254S, A296Y, N304H, G307S, A308Q , A308Q , G316A, L320T, K342V,
	Y354Q, E374C, S377Q, G378Y, Q393T*

Supplemental Table S7. Testing for the optimal amount of ligation mix to transform. Different amounts and dilutions of the ligation mix were transformed into XL1-Blue cells to test for effects of DNA and salt concentration on transformation efficiency. The most transformants results from transforming 4 uL of ligated fragments.



Dilution	Amount in transforma tion	Plate dilution	#Plaques	Titer (viruses /mL)
0	4 uL	1E-3	268	268,000
0	1 uL	1E-3,1E-2	23, 220	22,500
10X	1 uL	1E-2	57	5,700
100X	1 uL	1E-1	0	0
2X	1 uL (clean)	1E-3,1E-2	23, 99	16,450